The text that follows is a PREPRINT.

Please cite as:

dos Santos Junior, U.M., J.F.C. Gonçalves & P.M. Fearnside. 2012. Measuring the impact of flooding on Amazonian trees: photosynthetic response models for ten species flooded by hydroelectric dams. *Trees-Structure and Function*. (published online first 14 Apr. 2012)

doi:10.1007/s00468-012-0788-2

ISSN: 0931-1890 (print version) 1432-2285 (electronic version)

Copyright: Springer Science + Business Media, LLC

The original publication will be available at: http://www.springer.com

Measuring the impact of flooding on Amazonian trees: photosynthetic response models for ten species flooded by hydroelectric dams

Ulysses Moreira dos Santos Junior[a], José Francisco de Carvalho Gonçalves[a,]*, Philip Martin Fearnside[b]

[a] Laboratório de Fisiologia e Bioquímica Vegetal, Instituto Nacional de Pesquisas da Amazônia (MCT-INPA), Manaus, Amazonas, Brazil Tel.: +55 92 3643-1880.

[b] Coordenação de Pesquisas em Ecologia, Instituto Nacional de Pesquisas da Amazônia (MCT-INPA), Manaus, Amazonas, Brazil. Tel.: + 55 92 3643-1822. e-mail:pmfearn@inpa.gov.br

* Corresponding author: E-mail: jfc@inpa.com.br

22 January 2012
Revised 30 August 2012

Measuring the impact of flooding on Amazonian trees: photosynthetic response models for ten species flooded by hydroelectric dams

Abstract Increasing areas of Amazonian forest are coming under flood stress due to dam construction and greater variability in river flood levels due to climate change. The physiological responses of Amazonian trees subjected to flooding are important to understanding the consequences of these changes. Irradiance-response curves for photosynthesis obtained from ten tropical tree species growing in flooded areas were used to fit three empirical models. The study was done in floodplains along the Uatumã River, both upstream and downstream of the Balbina Hydroelectric Dam in Brazil's state of Amazonas (01° 55'S; 59° 28' W). Ten species were studied. Models compared were: non-rectangular hyperbola (NRH), rectangular hyperbola (RH) and exponential (EXP). All models were quantitatively adequate for fitting the response of measured data on photosynthesis to irradiance for all ten species in the non-flooding and flooding periods. Considerable variation was found among the model estimates of maximum photosynthesis (P_{nmax}), dark respiration (R_d) and apparent quantum yield of photosynthesis (α). For photosynthesis, the two hyperbolas overestimated P_{nmax} while EXP presented more realistic values. For estimating R_d, RH presented the most realistic values. To avoid unrealistic value estimates of R_d we recommend adding measured R_d values to the regressions. The results suggest that the EXP model presented the most realistic P_{nmax} and α values, and, in spite of less accuracy in fitting photosynthetic irradiance curves than the RH model, it can be recommended for accessing the information used in photosynthetic irradiance curves for the leaves of tropical trees growing in Amazonian floodplains or in areas that are artificially flooded by dams.

Keywords Apparent quantum yield – Carbon - Convexity term - Dark respiration – Global warming - Photosynthesis

Introduction

The carbon balance of Amazonian forests is a matter of global concern because any significant shift towards gain or loss would translate into climatically significant amounts of atmospheric carbon dioxide (Ometto et al. 2005). Forests gain or lose carbon as a result of a balance between rates of tree growth and recruitment on one side and mortality on the other. These rates are affected by the different stresses to which trees are subjected, such as lack of water, light or nutrients. One underappreciated stress in the context of Amazonian forests is that of flooding (Costa et al. 2009). The increased variability in river flow levels expected to result from projected climate changes indicates future increases in areas subject to flooding. The record-breaking Amazon floods of 2009, which even submerged part of downtown Manaus, offer a harbinger of this (Nobre and Borma 2009). Massive plans for dam building would subject additional forest areas to flood stress: Brazil's 2011-2020 electrical expansion plan (Brazil, MME 2011) calls for building 30 dams in the country's Amazon region by 2020, or one dam every four months. The physiological responses of Amazonian trees to stress from flooding are therefore important to understanding the consequences of these changes.

Tropical forests play an important role in regional and global CO_2 fluxes and could contribute up to 50% of total global primary productivity (Grace et al. 2001). Soil fertility differences are believed to explain a gradient of increasing net production from east to west in Amazonia (Malhi et al. 2006). Mature Amazonian forests can act either as sinks or sources, depending on climatic conditions, with droughts such as those during El Niño events resulting in net releases of carbon (Tian et al. 1998, 2000; Saleska et al. 2003; Rice et al. 2004; Davidson et al. 2012). Major Amazonian droughts in 2005 and 2010 caused by warm water in the Atlantic Ocean (rather than El Niño, which is triggered by warm water in the Pacific) dramatically stunted tree growth in the region (Phillips et al. 2009; Lewis et al. 2011). Both of these forms of drought are expected to increase in frequency and severity as a result of global warming (Cox et al. 2004, 2008). On the other hand, a major Amazonian flood occured during a La Niña event in 2009 that caused excess rainfall in the in the north and northeast of Amazon region (Marengo et al. 2011). Although the effect of drought dominates interannual variation in production in Amazonia as a whole, the effect of flooding is also an important factor in forest productivity.

Stress from flooding may play a substantial role in limiting the productivity of Amazonian forest trees. Current estimates indicate a large area of Amazonia that is subject to annual flooding. Traditionally, the annually flooded area in the Brazilian portion of the Amazon has been considered to be 70,000 km^2, or 2% of Brazil's share of the forest (Goulding 1980). Recently, synthetic-aperture radar (SAR) imagery from the Japanese Earth Resources Satellite (JERS), which can "see" through both clouds and tree cover to detect standing water on the forest floor, has produced much higher estimates, approximately 850,000 km^2 of forest (i.e., not counting savanna wetlands) being subject to flooding throughout the lowland Amazon in all of the countries that share the basin (Melack et al. 2004). This represents 17% of the forest, or an area more than double that of the US state of California. The areas affected by this "natural" flooding may increase as a result of hydrological impacts from land-use change (Costa et al. 2003) and climate change (Marengo et al. 2009).

Trees undergoing flooding stress are believed to halt or greatly reduce their rates of photosynthesis. At two forest sites located approximately 80 km North of Manaus and 100 km from the Balbina Dam, the Large-Scale Biosphere-Atmosphere (LBA) Project has measured CO_2 fluxes above the forest canopy from two 55-m high towers. Significantly lower carbon uptake at one of the two sites was ascribed to the larger area of seasonally flooded "*baixio*" (valley bottom) in the area surrounding the tower (Araújo et al. 2002).

The effect of "natural" flooding is now being joined by the effects of hydroelectric dams. Reservoirs fluctuate in water level, and at their peak water levels they temporally flood surrounding forest. Forests that are flooded permanently or for long periods of the year are killed, but those at slightly higher elevations that are only occasionally flooded for short periods will experience stress, killing some trees and slowing the growth of others. The raising of the water table in the forest surrounding the shoreline stresses trees even when pooled water at the surface is not present. For example, in the forest adjacent to the Samuel Reservoir in the state of Rondônia, in southwestern Amazonia, red dots visible on Landsat satellite imagery indicate this stressed forest (see Fearnside 2005). The Balbina Dam, where the current study was done, has several thousand km of shoreline, including the perimeters of approximately 3000 islands (e.g., Fearnside 1989). The forested portion of Brazilian Amazonia now has four "large" dams (Curuá-Una, Tucuruí, Balbina and Samuel) and three under construction (Belo Monte, Santo Antônio and Jirau). The only publically available long-range plan, independent of projected construction dates, indicates a total of 79 dams flooding 100,000 km^2 in Brazilian Amazonia (Brazil ELETROBRÁS 1987; see Fearnside 1995). The scale of these plans means that better tools are needed to assess dam impacts, including the impact of flooding stress on trees. Quantitative information on the effect of flooding on photosynthesis of tree species in these areas has been lacking and is supplied in the present paper for ten species. Identification of the best models for representing these impacts will facilitate future extension of the knowledge base relating flood stress to photosynthesis in tropical forest trees.

Several studies have been done to quantify the assimilation and emission of CO_2 by different forest types and by the different species that compose the forest ecosystems (Zhan et al. 2003; Oren et al. 2006; Stoy et al. 2006; Mercado et al. 2006). Models of photosynthesis play key roles in estimating primary production of vegetation under different conditions and have been used in ecosystem simulations and ecosystem modeling (Gao et al. 2004; Muraoka and Koizumi 2005). Complex mechanistic models of photosynthesis, such as the biochemical models of Farquhar et al. (1980) for C_3 leaves, have often been applied in studies of photosynthesis mechanisms (Peri et al. 2005). These models are usually derived from known quantitative relationships between different kinds of molecules involved in the biochemical processes of photosynthesis and require rather extensive calibration as well as complex parameterization (Cannell and Thornley 1998). Including a detailed representation of biochemical processes in the biochemical models is not always advantageous, as compared to the simpler leaf-photosynthetic models (Gao et al. 2004).

Due the complexity of mechanistic models, empirical models have been used to obtain information from irradiance-response curves of photosynthesis under different conditions (Sullivan et al. 1996; Eschenbach et al. 1998; Mielke et al. 2003; Morais 2003; Mielke and Schaffer 2010; Silva et al. 2011). Different models have been observed to produce large differences in estimates of important parameters obtained from photosynthesis-irradiance curves, such as maximum photosynthesis (P_{nmax}), dark respiration (R_d) and the apparent quantum yield of photosynthesis (α). These differences can cause errors in the interpretation of the data.

In spite of the differences among the models used in the literature, little attention has been paid to comparison of characteristics and behavior among models for estimating the main photosynthetic parameters. The goal of this study was to investigate the differences in estimates of the main photosynthetic parameters (P_{nmax}, R_d and α) produced by the three traditional models (non-rectangular hyperbola, rectangular hyperbola and exponential) and to analyze the three models by fitting measured data on photosynthesis in ten tropical tree species under flooding and non–flooding conditions.

Material and methods

Study area and species selection

The study was conducted in floodplains along the Uatumã River, both upstream and downstream of the Balbina hydroelectric dam, located about 220 km from Manaus in Presidente Figueiredo County, Amazonas state, Brazil (01^o 55'S; 59^o 28' W). The climate at this site is Amw under the Köppen classification system. In the period of the experiment (2005 – 2007) the annual average rainfall was 2392 mm and average values of minimum and maximum temperature were 23.3 and 33.9ºC, respectively. Monthly rainfall at the study location was obtained from Manaus Energia, the power company that operates the Balbina Dam. The physiological data were collected in two different periods (flooding and non-flooding). The non-flooding period was characterized by the reservoir water level varying between 47.64 and 48.21 m above mean sea level (January and February of 2006 and 2007) and the flooding period was characterized by the water level varying between 50.41 and 50.69 m (June and July of 2006 and 2007). The measurements of light curves were performed on ten plants for each of seven species

tolerant to flooding and for three non-tolerant species. After selection of the species in the field, fertile botanical material was collected for identification in the herbarium of the Instituto Nacional de Pesquisas da Amazônia (INPA). The flood-tolerant species were *Nectandra amazonum* Nees (Lauraceae), *Macrolobium angustifolium* (Benth.) Cowan (Caesalpiniaceae), *Alchornea discolor* Klotzch (Euphorbiaceae), *Brosimum lactescens* (S. Moore) C.C. Berg (Moraceae), *Senna reticulata* Willd. (Caesalpiniaceae), *Genipa spruceana* Steyerm. (Rubiaceae), *Parinari excelsa* Sabine (Chrysobalanaceae) and the non-tolerant species were *Cecropia concolor* Willd (Cecropiaceae), *Vismia guianensis* (Aubl.) Choisy (Clusiaceae)and *Vismia japurensis* Reichardt (Clusiaceae).

Photosynthetic measurements

Measurements of photosynthesis-irradiance (P_n-I) curves (or "light curves") were performed on healthy, completely expanded leaves in ten plants per species (ten species) in each period (flooding and non-flooding) from 7:30 to 16:30 h using a LI-6400 portable photosynthesis system (Li-cor, USA) equipped with an artificial irradiance source (6400-02B Red Blue). The P_n-I curves were derived using the "light curve" routine in the OPEN 3.4 software modified to accommodate eleven levels of photosynthetic photon flux density (PPFD: 0, 25, 50, 75, 100, 250, 500, 750, 1000, 1500, 2000 µmol quanta m^{-2} s^{-1}) in decreasing order. The minimum time allowed for the reading to stabilize at each PPFD level was 120 s, the maximum time for saving each reading was 300 s, and the maximum coefficient of variation (C.V.) was 1%. The Li-cor 6400 was adjusted to a flow rate of 400 µmol s^{-1}. The concentration of CO_2 (from a CO_2 cylinder mixed with atmospheric CO_2) was 380 µmol mol^{-1} and the concentration of H_2O vapor inside the assimilation chamber was 21 ± 3 mmol mol^{-1}. Block temperature was 31 ± 1°C. Before each measurement the leaves were exposed to 1000 µmol (quanta) m^{-2} s^{-1} for an adaptation period of 5 to 10 min, after which the measurements of the P_n-I curves were performed.

Description of the models

Three empirical models were tested: (1) Non-rectangular hyperbola (Marshall and Biscoe, 1980), (2) Rectangular hyperbola (Thornley 1976) and (3) Exponential (Iqbal et al. 1997) (Table 1).

In the models: I is the irradiance (~PPFD); P_n is the rate of net photosynthesis (µmol CO_2 m^{-2} s^{-1}); P_{nmax} is the maximum photosynthesis; R_d is dark respiration (µmol CO_2 m^{-2} s^{-1}) corresponding to the value of P_n when I = 0 µmol m^{-2} s^{-1}; θ is a dimensionless convexity term, and α is the apparent quantum yield of photosynthesis (mol CO_2 mol $quanta^{-1}$).

A non-rectangular hyperbola (NRH) was fitted according to Model 1 (Table 1). To avoid correlation between α and θ during curve fitting, α was first found by least-squares regression of the initial linear portion of curve, including darkness (PPFD between 0-100 µmol m^{-2} s^{-1}). The result of the Kok effect in estimates of α was analyzed in this study. For rectangular hyperbolas and exponential models α was estimated with the non-linear curves.

In this study two situations were analyzed. In the first the estimated parameters were R_d, P_{nmax} and α or θ, depending of the model used. In the second a measured dark respiration (R_d) term was added to the model and only P_{nmax} and α or θ were estimated by the models. The "measured" α was estimated by linear regression of P_n on PPFD between 0-100 µmol m^{-2} s^{-1}; the measured R_d was considered to be the value of CO_2 flux when when PPFD = 0 µmol m^{-2} s^{-1}, and the measured P_{nmax} was considered to be the mean value of P_n when PPFD ≥ 1500 µmol m^{-2} s^{-1}.

Statistical analysis

Every model was fitted to measured data from each of the 200 P-I curves using the Levemberg-Marquardt algorithm in the non-linear least-squares estimation routine in the Statistica for Windows (Version 6.0) software (StatSoft Inc., Tulsa, OK, USA). The initial values for P_{nmax}, R_d, α and θ were set at 10 µmol CO_2 m^{-2} s^{-1}, 0.1 µmol CO_2 m^{-2} s^{-1}, 0.01 mol CO_2 mol^{-1} photons and 0.1, respectively, making them coherent with the predicted values. None of the initial values for P_{nmax}, R_d, α and θ were modified.

For each model, the goodness of fit was verified by plotting the modeled curve against the mean of ten measured curves for each species, based on the analysis of residuals, the coefficient of determination (r^2), the average of unsigned deviation (*Aud*) and the root mean square of error (*RMSE*). The r^2 value was used to evaluate the amount of variation explained by a regression; this statistic is commonly used to select the best regression. Due the r^2 giving heavy weight to observations with large magnitudes, an additional loss function was used to verify the best fit: average of unsigned deviation (*Aud*% = Σ (|(Predicted-measured)|/measured) x 100/n)). As an alternative statistic to confirm the best goodness of fit for the models, the root mean square error (*RMSE*), or $\sqrt{\Sigma Error^2/n}$, was reported.

Results

Comparison of the fits and of the estimates of P_{nmax}, R_d, α and θ produced by the models

All three models were adequate ($P < 0.013$ for all species in the two periods) and showed high coefficients of determination ($r^2 > 0.94$) for all species in both the non-flooding (NFP) and flooding (FP) periods (Table 2). Comparing the goodness of fit of the models, RH generally had the best fit as shown by the lower values of average unsigned deviation (*Aud*%) and root mean square error (*RMSE*) for all of the species studied (Table 2). NRH produced the worse fit.

The three models showed a random distribution of residuals around the predicted values for all species in both periods (Fig. 1). The RH model presented the lowest values of residuals for all levels of PPFD, as compared to the NRH and EXP models (Fig. 1). In general, the NRH and EXP models presented an underestimation of P_n at PPFD = 0, 25, 500, 750 and 1000 μmol m^{-2} s^{-1} and an overestimation of P_n at PPFD = 50, 75, 100, 250, 1500 and 2000 μmol m^{-2} s^{-1} (Fig. 1).

In Fig. 2 estimates of maximum net photosynthesis (P_{nmax}), predicted dark respiration (R_d) and predicted apparent quantum yield of photosynthesis (α) as calculated by the models are plotted against the measured values for 200 plants from ten species and two periods (non-flooding and flooding). The best estimate of P_{nmax} was presented by the EXP model while the two hyperbolas overestimated the values of P_{nmax} (Fig. 2A-B; Table 3). NHR exhibited values of predicted P_{nmax} higher than measured P_{nmax} , varying, depending on the species, from 33.7 to 80.5% (*NFP*) and from 7.3 to 62.4% (*FP*). RH presented values of P_{nmax} that were higher than the measured P_{nmax} by 11 to 31.1% (*NFP*) and by 5.2 to 36.9% (*FP*) (Table 3). On the other hand, the EXP model presented good estimates of P_{nmax} for all species, presenting a slight underestimation. In addition, EXP showed the best correlation between measured and predicted values of P_{nmax}, while NHR showed the worse. For R_d RH presented a good estimate, with mean overestimates of 5.8% (*NFP*) and 9.9% (*FP*) for all species (Table 4). On the other hand, NRH and EXP exhibited a clear underestimation of R_d. In addition, all of the models showed negative values of predicted R_d, indicating problems for interpretation of these data (Fig. 2C-D).

The α value estimated by linear regressions with exclusion of points from the Kok-effect region (PPFD < 20 μmol m^{-2} s^{-1}) had mean underestimations of 7.6% (*NFP*) and 8.9% (*FP*) as compared to measured α (PPFD 0-100 μmol m^{-2} s^{-1}) (Table 5). The α estimated by the RH models was, on average, 43.8 (*NFP*) and 70.0% (*FP*) higher than the measured α, and for the EXP models the estimated values of α underestimated by 1.2% for the flooding period and overestimated by 13.8% for the non-flooding period compared to measured α values, considering all species (Table 5).

Comparison of the fits and of the estimate P_{nmax}, α and θ by the models when R_d values from measured data were added to the models.

When the measured data on R_d were added to the models for estimation of P_{nmax} and α, the accuracy for all models decreased as compared to the models in which estimated values of R_d were used, as demonstrated by decreasing r^2 values and increasing *RMSE* values (compare the values in Tables 2 to 6). However, the models were adequate ($P < 0.01$ for all species and both periods) in the models in which R_d values were estimated.

The analyses of residuals showed higher values than the residuals from the models in which R_d was estimated, especially for NRH (Fig. 3). The RH model continued showing the lowest values for residuals for all levels of PPFD (Fig. 3). The distribution of the residuals showed that the NRH and EXP models overestimated P_n at PPFD = 25 μmol m^{-2} s^{-1}, while the models in which R_d was estimated presented an underestimates (Compare Fig. 3 to Fig. 1).

In Fig. 4, estimates of maximum net photosynthesis (P_{nmax}) and predicted apparent quantum yield of photosynthesis (α) when Rd was added to the models (as calculated by the models) are plotted against the measured for 200 plants from ten species and two periods (non-flooding and flooding). For the estimated parameters a better estimation of P_{nmax} by NRH was found when R_d was added, as compared to the situation in which R_d was estimated by the NRH model (Compare values of Table 7 to Table 3). For the RH and EXP models a slight difference was observed, in which the EXP model showed more realistic estimates of P_{nmax}, as compared to the two hyperbola models. For α, RH and EXP models presented better linear correlations between measured and estimated values of α, with higher values of r^2 when measured R_d was included in the models (Table 8). In addition, EXP models presented more realistic estimates of α as compared to RH models. For θ in NRH models, on average, underestimates of 7.0% (*NFP*) and 4.5% (*FP*) were observed when measured R_d was added to the models, considering all species (Table 9).

Discussion

Models fit performance

In this study all three models were quantitatively adequate ($P < 0.013$) in predicting the behavior of the photosynthesis irradiance curves for each species in each period. Similar results were found by Gomes et al. (2006), in which NHR, RH and EXP models were found to be quantitatively adequate for dwarf coconut. To evaluate the best quantitative performance among the three models the values of r^2, *Aud*% and *RMSE* were observed. Higher values of r^2 and lower values of *Aud*% and *RMSE* for RH may indicate better accuracy and quantitative performance compared to the other two models for the majority of the species studied in the two periods, especially for NRH models. Some studies have used the *F*-test to compare the variability of predictions with the variability of measured data with lower absolute values of F indicate better quantitative performance (Pachesky et al. 1996; Gomes et al. 2006). Using the *F*-test, Gomes et al. (2006) concluded that EXP models had better quantitative performance than the two hyperbolas.

Analyses of residuals confirmed the results shown by the *Aud*% and *RMSE* values, indicating that RH model presented the better goodness of fit than EXP and NRH models. On the other hand, NHR model showed the highest residuals around the predicted values of P_n, except for *C. concolor* in the non-flooding period (Fig 1). For *S. reticulata* (*NFP* and *FP*) and *C. concolor* (*NFP*), the high values of residuals may be the result of the high values of P_n that these species exhibited. It is interesting to observe that in some PPFD for some species the behavior of residuals for RH was different from the NHR and EXP models. Therefore, while RH models showed an overestimation of residual values, NHR and EXP models showed underestimations of the values of residuals (see *N. amazonum*, *G. spruceana*, Fig. 1).

P_{nmax} performance

Estimates of P_{nmax} varied depending on the model used. The best estimation was presented by the EXP model, while NRH and RH models resulted in large overestimations. A similar result was found by Gomes et al. (2006), who concluded that P_{nmax} was more realistic when estimated by the EXP model. The good estimation of P_{nmax} by the EXP model suggests that this empirical model can be used as a submodel for predicting values in productivity models and for environmental modeling of the CO_2 balance.

R_d performance - part 1

The most realistic estimation of R_d was obtained from the RH model, while the EXP and NRH models presented a high underestimates. The underestimation of R_d can be substantial, as observed in this study for some plants, and the estimated values can be unrealistic (see Fig. 2C-D), with the estimates of R_d values reaching negative values (for the models, R_d present positive values). Similar results were found by Vervuren et al. (1999), who observed that R_d was negative in some cases, suggesting unrealistic estimates of respiratory oxygen production. This fact can be problematic for the interpretation and comprehension of the CO_2 balance in single plants and even more so for vegetation.

α performance

The calculation of α varied among the three models tested. First the Kok-effect region was analyzed in the estimation of α. The α value is estimated from the initial slope of the linear regression of the P_n – I curves, where the net photosynthesis is linear with increasing irradiance. In this study, exclusion of points from the Kok effect region (Sharp et al., 1984) was found to promote, on average, an underestimation of 7.6% (*NFP*) and 8.9% (*FP*) of α as compared to the α estimated from initial slope including points in the Kok-effect region (e.g., PPFD = 0 μmol m^{-2} s^{-1}). Similar results were observed by Clearwater et al. (1999) and Gonçalves and Santos Junior (2005), who found differences of 10 and 12.5%, respectively. According Leverenz (1987), this difference occurs due to increases in mitochondrial respiration at very low irradiance (PPFD < 20 μmol m^{-2} s^{-1}). The inclusion of the points from the Kok-effect region is responsible for increasing the angular coefficient (slope) of the linear regression from the initial slope and, consequentially, increasing the α values.

When α was estimated by the RH model a substantial overestimation was observed as compared to measured α values (or linearly estimated from PPFD ~ 0-100 μmol m^{-2} s^{-1}). This overestimation by RH has been demonstrated in many studies (Mielke et al. 2003; Gomes et al. 2006). In addition, Hootsman and Vermaat (1991) found a satisfactory goodness of fit for the RH model, however, on the basis of the consistent parameter overestimation of P_{nmax} and α as observed by Vervuren et al. (1999) and Iwakuma and Yasuno (1983), application of the RH model was considered inappropriate by these authors. For the EXP model substantial overestimation of α was found, on average, for the species in the flooding period, especially for *C. concolor*, *V. guianensis* and *V. japurensis*, that presented low values of α. These results indicated that the RH and EXP models presented higher overestimation for low values of α. The linear correlation between α values estimated by RH and EXP models for all species together was higher ($r^2 > 0.92$, data not shown) as compared to the correlation between measured α values and α values estimated by the RH model ($r^2 > 0.57$) and the EXP model ($r^2 > 0.647$) (see Table 4), indicating that the principles for calculating α by RH and EXP models are similar.

Theoretically, the maximum value that α can reach is 0.125 mol mol^{-1}, meaning that 8 moles of photons are required to reduce 1 mole of CO_2 in the absence of photorespiration (Singsaas et al. 2001). However, due to

cyclic photophosphorylation, the maximum α value may be closer to 0.112 in most C_3 plants). Comparing the estimating α by the models, RH model presented values closer to the theoretical maximum α. However, the α values estimated by the models were much lower than the theoretical maximum. These results have been found by many researchers in the context of a large set experiments with many different species, with reported values 30-85% lower than the 0.125 mol mol^{-1} theoretical maximum (Clearwater et al. 1999, Marenco et al. 2001a,b; Singsaas et al. 2001; Santos Junior 2003; Gonçalves et al, 2005). The low values of α may be the result of unfavorable environmental factors (e.g. drought, flooding, high irradiance) and/or may originate from physiological processes that compete with CO_2 reduction, such as photoinhibition that provokes damage to the photosynthetic apparatus (Groom and Baker 1992; Gonçalves et al. 2005), photorespiration (Sharkey 1988; Peterson 1990; Singsaas et al. 2001) and alternative competitors such as NO^-_3 and oxygen reduction outside of the photorespiration process (Edwards and Walker 1983; Robinson 1988; Cornic and Briantais 1991).

Thus, for estimates of α, all models are adequate. However, one must avoid comparing values of α calculated by different models; in other words, when researchers compare their results to those of others they must pay close attention to how the α values were estimated.

R_d performance - part 2

To avoid problems in estimation of R_d (see discussion above), measured R_d values were included in the models and only P_{nmax} and α or θ were estimated by the models. This solution has been used by some researchers to avoid problems with the underestimation of R_d (Clearwater et al. 1999; Vervuren et al. 1999; Gonçalves et al. 2005). When R_d was included in the models the regressions, on average, lose accuracy as compared to the situation in which R_d was estimated, as indicated by the decrease of r^2 values and the increase of *Aud*% (except for RH models in the non-flooding period) and *RMSE*. The loss of accuracy was most evident in the NRH model. This result was confirmed by the analysis of residuals in which the NRH model presented higher values of residuals as compared to the RH and EXP models. This indicates that use of the NRH model may provoke much more error in modeling the photosynthetic irradiance response than the RH and EXP models. In addition, it is clear that, in spite of NRH having been frequently used by many researchers, for the species in this study its presented the worse quantitative performance, as compared to the RH and EXP models.

For estimation of P_{nmax}, the EXP models continued presenting the most realistic estimates as compared to the two hyperbolic models, suggesting that the EXP models are most adequate for estimating P_{nmax} in both situations. EXP also presented better estimates for α than did the RH models. These results suggest that the main problem presented by the EXP model is in estimating R_d, because for P_{nmax} and α, the EXP model presented the best estimation.

Convexity term (θ) performance in non-rectangular hyperbola

For estimating the convexity term (θ), mean values of 0.838 (NFP) and 0.884 (FP) were observed (Table 9). When measured values of R_d were added to the models, the estimated θ increased, on average, by 7.0 and 4.5% for the non-flooding and flooding periods, respectively. These results were higher than the θ values observed by Thomas and Bazzaz (1999) in a study of dipterocarp species (θ value ranging from 0.20 to 0.80). On the other hand, Santos Junior (2003) and Gonçalves et al. (2005) found values of θ ranging from 0.85 to 0.97 for tree species in Amazonian forest. The low and high values of θ are related to gradual and abrupt transitions, respectively, in the light curve, between the region where irradiance is limiting and the region where irradiance is saturated (Thornley 1998). The convexity term has been related to irradiance saturation in chloroplasts, and factors such as irradiance, stress conditions, pigment content and foliar morphology may affect the θ value (Leverens 1987; Hirose and Werger 1987; Evans 1993; Ogren 1993; Kull and Niinementes 1998).

Conclusions

In this study all three models were quantitatively adequate for fitting the response of measured data of photosynthesis to irradiance, in all ten species in the non-flooding and flooding periods. However, RH and EXP were more adequate than NRH in both situations in which R_d was estimated or in which the measured R_d was added to the regression. For parameter estimation, considerable variation was found among estimates of P_{nmax}, R_d and α among the models. These differences must be considered in the interpreting the data and in making comparisons with the results of other researchers. For photosynthesis, the two hyperbolas overestimate P_{nmax} while EXP presented more realistic values. Considering the estimation of R_d, the RH model presented the most realistic values, as compared to the NRH and EXP models. However, all models presented problems to estimate R_d, because for any plants the estimated values were biologically impossible to explain. To avoid this situation, especially for the NRH and EXP models, the solution is to add the measured R_d term to the regression. When the R_d term was added, EXP presented the most realistic estimation of P_{nmax} and α, as compared to the RH, and NRH models, which continued to overestimate P_{nmax}. Thus, we conclude that: a) R_d should be added to the regressions to avoid problems of unrealistic estimated values of R_d; b) The NRH model, in spite of being frequently used,

was less accurate in fitting the photosynthetic irradiance-curves and performed poorly in estimating P_{nmax}, as compared to the RH and EXP models; c) The RH model presented the best accuracy to fitting the photosynthetic irradiance-curves and can be recommended for adjusting the light curves. However, the RH models presented problems to overestimated P_{nmax} and α; d). The EXP model presented most realistic P_{nmax} and α values and, in spite of showing less accuracy in fitting photosynthetic-irradiance curves than the RH model, this model can be recommended for accessing photosynthetic irradiance curves for the leaves of tropical trees growing in Amazon floodplains or in artificially flooded areas, such as dams. These curves constitute a key tool for understanding the impact of flooding on carbon balance in Amazonian forests that are being increasingly subjected to stress from flooding.

Acknowledgements

We thank the Conselho Nacional de Desenvolvimento Científico e Tecnológico (CNPq); the Fundação de Amparo à Pesquisa do Estado do Amazonas (FAPEAM), the Large-Scale Atmosphere-Biosphere Experiment in Amazonia (LBA), the Instituto Chico Mendes (ICMBio), the Manaus Energia, The IBAMA and the entire team of the Laboratory of Plant Physiology and Biochemistry. J.F.C Gonçalves and P.M. Fearnside acknowledge fellowships provided by CNPq.

References

Araújo AC, Nobre AD, Kruijt B, Dallarosa R, Elbers J, Stefani P, Von Randow C, Manzi AO, Gash JHC, Kabat P (2002) Comparative measurements of CO_2 exchange for two towers in an Amazonian rainforest: The LBA Manaus site. Journal of Geophysical Research 107(D20) doi: 10.1029/2001JD000676

Brazil, ELETROBRÁS (1987) Plano 2010: Relatório Geral. Plano Nacional de Energia Elétrica 1987/2010 (Dezembro de 1987). Centrais Elétricas do Brasil (ELETROBRÁS), Brasília, DF, Brazil.269 pp.

Brazil, MME (2011) Plano Decenal de Expansão de Energia 2020. MME (Ministério de Minas e Energia), Empresa de Pesquisa Energética. Brasília, DF, Brazil. 2 vols.

Cannell MGR, Thornley JHM (1998) Temperature and CO_2 responses of leaf and canopy photosynthesis: a clarification using the non-rectangular hyperbola model of photosynthesis. Ann Bot 82:883-892

Clearwater MJ, Susilawaty R, Efendi R, Gardingen PR (1999) Rapid photosynthetic acclimation of Shorea johorensis seedlings after logging disturbance in Central Kalimantan. Oecologia 121:478-488.

Cornic G, Briantais J (1991) Partitioning of photosynthetic electron flow between CO_2 and O_2 reduction in a C_3 leaf (*Phaseolus vulgaris* L.) at different CO_2 concentration and during drought stress. Planta 183:178-184.

Costa MH, Botta A, Cardille JA (2003) Effects of large-scale changes in land cover on the discharge of the Tocantins River, southeastern Amazonia. Journal of Hydrology 283:206–217.

Costa, MH, Coe, MT, Guyot, JL (2009) Effects of climatic variability and deforestation on surface water regimes. In: Keller M, Bustamante M, Gash J, da Silva Dias P (Eds.), Amazonia and Global Change. Geophysical Monograph Series, Volume 186, American Geophysical Union (AGU), Washington, DC, U.S.A., pp. 543-553.

Cox PM, Betts RA, Collins M, Harris PP, Huntingford C, Jones CD (2004) Amazonian forest dieback under climate-carbon cycle projections for the 21st century. Theor Appl Climatol 78:137-156.

Cox PM, Harris PP, Huntingford C, Betts RA, Collins M, Jones CD, Jupp TE, Marengo JA, Nobre CA (2008) Increasing risk of Amazonian drought due to decreasing aerosol pollution. Nature 453:212-215.

Davidson EA, Araújo AC, Artaxo P, Balch JK, Brown JF, Bustamante MMC, Coe MT, Defries RS, Keller M, Longo M, Munger JW, Schroeder W, Soares-Filho BS, Souza Jr CM, Wofsy SC (2012) The Amazon Basin in Transition. Nature 481:321-328

Edwards E, Walker D (1983) C_3, C_4: mechanisms, and cellular and environmental regulation, of photosynthesis. Blackwell, Oxford.

Evans JR (1993) Photosynthetic acclimation and nitrogen partitioning within theoretical optimum. Aust J Plant Physiol 20:69-82.

Eschenbach C, Glauner R, Kleine M, Kappen L (1998) Photosynthesis rates of selected tree species in lowland dipterocarp rainforest of Sabah, Malaysia. Trees 12:356-365.

Farquhar GD, von Caemmerer S, Berry JA (1980) A biochemical model of the photosynthetic CO_2 assimilation in leaves of C_3 species. Planta 149:78-90.

Fearnside PM (1989) Brazil's Balbina Dam: Environment versus the legacy of the pharaohs in Amazonia. Environmental Management 13:401-423.

Fearnside PM (1995) Hydroelectric dams in the Brazilian Amazon as sources of 'greenhouse' gases. Environmental Conservation 22:7-19.

Fearnside PM (2005). Brazil's Samuel Dam: Lessons for hydroelectric development policy and the environment in Amazonia. Environmental Management 35:1-19.

441 Gao Q, Zhang X, Huang Y, Xu H (2004) A comparative analyses of four models of photosynthesis for 11 plant
442 species in the Loess Plateau. Agricultural and Forest Meteorology 126:203-222.
443 Gomes FP, Oliva MA, Mielke MS, Almeida A-AF, Leite HG (2006) Photosynthetic irradiance-response in
444 leaves of dwarf coconut palm (Cocos nucifera L. "nana", Araceae): Comparison of three models.
445 Scientia Horticulture 109:101-105.
446 Gonçalves JFC, Barreto DCS, Santos Junior UM, Fernandes AV, Sampaio PTB, Buckeridge MS (2005) Growth,
447 photosynthesis and stress indicators in young rosewood plants (Aniba rosaeodora Ducke) under
448 different light intensities. Braz J Plant Physiol 17:325-334.
449 Gonçalves JFC, Santos Junior UM (2005) Assimilação de carbono e indicadores de estresse da Amazônia. In:
450 Nogueira, RJMC, Araújo EL, Willadino LG, Cavalcante, UMT (Ed). Estresses ambientais: danos e
451 benefícios em plantas. Recife: UFRPE, Imprensa Universitária; p. 500 (Chapter 15:165-181 ISBN 85-
452 87459-20-1).
453 Goulding M (1980) The Fishes and the Forest: Explorations in Amazonian Natural History. University of
454 California Press, Berkeley, 280 pp.
455 Grace J, Malhi Y, Higuchi N, Meir P (2001) Productivity and carbon fluxes of tropical rain forest. In: Roy HAM
456 (Ed). Global Terrestrial Productivity. Academic Press, San Diego.
457 Groom QJ, Baker NR (1992) Analysis of light-induced depressions of photosynthesis in leaves of a wheat crop
458 during the winter. Plant Physiol 100:1217-1223.
459 Hirose T, Werger MJA (1987) Nitrogen use efficiency in instantaneous and daily photosynthesis of leaves in
460 canopy of a Solidago altissima stand. Physiol Plant 70:215-222.
461 Hootsman MJM, Vermaat JE (1991) Light-response curves of Potamogeton pectinatus L. as a function of plant
462 age and irradiance level during growth. In Macrophytes, a key to understanding changes caused by
463 eutrophication in shallow freshwater ecosystems. pp. 57-130. PhD Thesis. International Institute for
464 Hydraulic and Environmental Enginneering. Delft.
465 Iqbal RM, Rao A-R, Rasul E, Wahid A (1997) Mathematical models and response functions in photosynthesis:
466 an exponential model. In: Pessarakli M. (Ed.), Handbook of photosynthesis. Marcel Dekker Inc., New
467 York, U.S.A., pp. 803–810.
468 Iwakuma T, Yasuno M (1983) A comparison of several mathematical equations describing photosynthesis-light
469 curve for natural phytoplankton population. Archiv fur Hydrobiologie 97:208-226.
470 Kull O, Niinemets U (1998) Distribution of leaf photosynthetic properties in tree canopies: comparison of
471 species with different shade tolerance. Funct Ecol 12:472-479.
472 Leverenz JW (1987) Chlorophyll content and the light response curve of shade-adapted conifer needles. Physiol
473 Plant 71:20-29.
474 Lewis SL, Brando PM, Phillips OL, van der Heijden GMF, Nepstad D (2011) The 2010 Amazon drought.
475 Science 331:554.
476 Malhi Y, Wood D, Baker TR, Wright J, Phillips OL, Cochrane T, Meir P, Chave J, Almeida S, Arroyo L,
477 Higuchi N, Killeen T, Laurance SG, Laurance WF, Lewis SL, Monteagudo A, Neill DA, Vargas PN,
478 Pitman NCA, Quesada CA, Salomão R, Silva JNM, Lezama AT, Terborgh J, Martínez RV, Vinceti B
479 (2006) The regional variation of aboveground live biomass in old-growth Amazonian forests. Global
480 Change Biol 12:1107-1138.
481 Marenco RA, Gonçalves JFC, Vieira G (2001a). Leaf gas exchange and carbohydrates in tropical trees differing
482 in successional status in two light environments in central Amazonia. Tree Physiol 21:1311-1318.
483 Marenco RA, Gonçalvez JFC, Vieira G (2001b) Photosynthesis and leaf nutrient contents in Ochroma
484 pyramidale (Bombacaceae). Photosynthetica 39:539-543.
485 Marengo JA, Jones R, Alves LM, Valverde MC (2009) Future change of temperature and precipitation extremes
486 in South America as derived from the PRECIS regional climate modeling system. International Journal
487 of Climatology 30:1-15.
488 Marengo JA, Tomasella J, Soares WR, Alves LM, Nobre CA (2011) Extreme climatic events in Amazon basin:
489 Climatological and hydrological context of recent floods. Theor Appl Climatol DOI 10.1007/s00704-
490 011-0465-1.
491 Marshall B, Biscoe PV (1980) A model for C_3 leaves describing the dependence of net photosynthesis on
492 irradiance. J Exp Bot 31:29–39.
493 Melack JM, Hess LL, Gastil M, Forsberg BR, Hamilton SK, Lima IBT, Novo EMLM (2004) Regionalization of
494 methane emissions in the Amazon Basin with microwave remote sensing. Global Change Biol 10:530-544.
495 Mercado L, Lloyd J, Carswell F, Malhi Y, Meir P, Nobre AD (2006) Modelling Amazonian forest eddy
496 covariance data: a comparison of big leaf versus sun/shade models for C-14 tower at Manaus I. Canopy
497 photosynthesis. Acta Amazonica 36:69-82.
498 Mielke MS, Schaffer B (2010) Leaf gas exchange, chlorophyll fluorescence and pigment indexes of Eugenia
499 uniflora L. in response to changes in light intensity and soil flooding. Tree Physiol 30:45-55.

500 Mielke MS, Almeida A-AF, Gomes FP, Aguilar MAG, Mangabeira PAO (2003) Leaf gas exchange, chlorophyll
501 fluorescence and growth responses of Genipa americana seedlings to soil flooding. Environ Exp Bot
502 50:221-231.
503 Morais RR (2003) Ecofisiologia de espécies arbóreas crescidas sob condições de plantios na Amazônia central.
504 Manaus, INPA/UFAM, 158 p.
505 Muraoka H, Koizumi H (2005) Photosynthetic and structural characteristics of canopy and shrub trees in a cool-
506 temperate deciduous broadleaved forest: Implication to ecosystem carbon gain. Agricultural and Forest
507 Meteorology 134:39-59.
508 Nobre CA, Borma LS (2009) 'Tipping points' for the Amazon forest. Current Opinion in Environmental
509 Sustainability 1:28-36. Doi:10.1016/j.cosust.2009.07.003.
510 Ogren E (1993) Convexity of the photosynthetic irradiance-response curve in relation to intensity and direction
511 of irradiance during growth. Plant Physiol 101:1013-1019.
512 Ometto JP, Nobre AD, Rocha H, Artaxo P, Martinelli L (2005) Amazônia and the modern carbon cycle: Lessons
513 learned. Oecologia 143:483-500.
514 Oren R, Hsieth CI, Stoy PC, Albertson J, McCarthy HR, Harrell P, Katul GG (2006) Estimating the uncertainty
515 in annual net ecosystem carbon exchange: spatial variation in turbulent fluxes and sampling errors in
516 eddy-covariance measurements. Global Change Biol 12:883-896.
517 Pachesky LB, Hesketh JD, Acock B (1996) An adequate model of photosynthesis I. Parameterization, validation
518 and comparison of models. Agric Syst 50:209-225.
519 Peri PL, Moote DJ, McNeil DL (2005) Modelling photosynthetic efficiency (α) for the light-response curve of
520 cocksfoot leaves grown under temperate field conditions. Eur J Agron 22:277-292.
521 Peterson RB (1990) Effects of irradiance on the in vivo CO_2:O_2 specificity factor in tobacco using simultaneous
522 gas exchange and fluorescence techniques. Plant Physiol 94:892-898.
523 Phillips OL, and 65 others (2009) Drought sensitivity of the Amazon rainforest. Science 323:1344-1347.
524 Rice AH, Pyle EH, Saleska SR, Hutyra L, Palace M, Keller M, de Camargo PB, Portilho K, Marques DF, Wofsy
525 SC (2004) Carbon balance and vegetation dynamics in an old-growth Amazonian forest. Ecological
526 Applications 14 Supplement: S55-S71.
527 Robinson J (1988) Does O_2 photoreduction occur within chloroplasts in vivo? Physiol Plant 72:666-680.
528 Saleska SR, Miller SD, Matross DM, Goulden M, Wofsy SC, da Rocha HR, de Camargo PB, Crill P, Daube BC,
529 de Freitas HC, Hutyra L, Keller M, Kirchoff V, Menton M, Munger JW, Pyle EH, Rice AH, Silva H
530 (2003). Carbon in Amazon forests: Unexpected seasonal fluxes and disturbance-induced losses. Science
531 302:1554-1557
532 Santos Junior UM (2003) Ecofisiologia de espécies arbóreas plantadas sobre área degradada por atividade
533 petrolífera na Amazônia Central. INPA/UFAM, Manaus, Amazonas, 135 pp.
534 Sharkey TD (1988) Estimating the rate of photorespiration in leaves. Physiol Plant 73:666-680.
535 Sharp RE, Mathews MA, Boyer JS (1984) Kok effect and the quantum yield of photosynthesis: light partially
536 inhibits dark respiration. Plant Physiol 75:95-101.
537 Singsaas EL, Ort DR, DeLucia EH (2001) Variation in measured values of photosynthetic quantum yield in
538 ecophysiological studies. Oecologia 128:15-23.
539 Silva CEM, Gonçalves JFC, Alves EG (2011) Photosynthetic traits and water use species growing on abandoned
540 pasture in diferent periods of precipitation in Amazonia. Photosynthetica 49:246-252.
541 Stoy PC, Katul GG, Siqueira MBS, Juang J-Y, Novick KA, Uebelherr JM, Oren R (2006) Agricultural and
542 Forest Meteorology 141:2-18.
543 Sullivan NH, Bolstad PV, Vose JM (1996) Estimates of net photosynthetic parameters for twelve tree species in
544 mature forests of the southern Appalachians. Tree Physiol 16:397-406.
545 Thomas SC, Bazzaz FA (1999) Asymptotic height as predictor of photosynthetic characteristics in Malaysian
546 rain forest trees. Ecology 80:1607-1622.
547 Thornley JHM (1976) Mathematical models in plant physiology, A quantitative approach to problems in plant
548 and crop physiology. Academic Press, London.
549 Thornley JHM (1998) Dynamic model of leaf photosynthesis with acclimation to light and nitrogen. Annals of
550 Botany 81:421-430.
551 Tian HQ, Melillo JM, Kicklighter DW, McGuire AD, Helfrich JVK III, Moore, BIII, Vörösmarty CJ (1998)
552 Effect of interannual climate variability on carbon storage in Amazonian ecosystems. Nature 396:664-
553 667.
554 Tian HQ, Melillo JM, Kicklighter DW, McGuire AD, Helfrich III J, Moore III B, Vorosmarty CJ (2000)
555 Climatic and biotic controls on annual carbon storage in Amazonian ecosystems. Global Ecology and
556 Biogeography 9:315–335.
557 Vervuren PJA, Beurskens SMJH, Blom CWPM (1999) Light acclimation, CO_2 response and long-term capacity
558 of underwater photosynthesis in three terrestrial plant species. Plant Cell Environ 22:959-968.

559 Zhan X, Xue Y, Collatz GJ (2003) An analytical approach for estimating CO_2 and heat fluxes over the
560 Amazonian region. Ecological Modelling 162:97-117.
561
562 **LEGENDS**
563
564 **Figure 1**. Residuals (measured minus predicted values) for net photosynthesis (P_n) obtained after adjusting the
565 non-rectangular hyperbola (white), the rectangular hyperbola (black) and the exponential (gray) models to the
566 field data of irradiance curves of photosynthesis, when dark respiration (R_d) was estimated by the models, in ten
567 tropical tree species in flooding (right) and non-flooding (left) periods.
568
569 **Figure 2**. Predicted and measured values of the maximum net photosynthesis (P_{nmax}, A-B), dark respiration (R_d,
570 C-D) estimated by the models and apparent quantum yield (α, E-F) in ten tropical tree species in non-flooding
571 (A, C, E) and flooding (B, D, F) periods.
572
573 **Figure 3**. Residuals for net photosynthesis (P_n) values obtained after adjusting the non-rectangular hyperbola
574 (white), the rectangular hyperbola (black) and the exponential (gray) models to field data on irradiance curves of
575 photosynthesis, when measured dark respiration (R_d) is included in the models, in ten tropical tree species in
576 flooding and non-flooding periods. *The residual value for P_n was 0 at PPFD = 0 μmol m^{-2} s^{-1} because, in this
577 situation, the estimated R_d is equal the R_d from measured data.
578
579 **Figure 4**. Predicted and measured values of the maximum net photosynthesis (P_{nmax}, A-B), apparent quantum
580 yield (α, C-D) and convexity term (θ) in ten tropical tree species in non-flooding (A, C, E) and flooding (B, D, F)
581 periods. *Dark respiration was not estimated by the models because the measured R_d was added to the models.
582

583
584 **Table 1**. Non-linear photosynthesis-irradiance models

Model number	Description	Model
1	Non-rectangular hyperbola (NRH)	$P_n = \{[(\alpha I + P_{nmax} + R_d) - ((\alpha I + P_{nmax} + R_d)^2 - 4\alpha I\theta(P_{nmax} + R_d))^{0.5}]/2\theta\} - R_d$
2	Rectangular hyperbola (RH)	$P_n = \alpha I(P_{nmax} + R_d)/ [\alpha I + (P_{nmax} + R_d)] - R_d$
3	Exponential (EXP)	$P_n = (P_{nmax} + R_d) \{1-\exp[-\alpha I/(P_{nmax} + R_d)]\} - R_d$

585
586
587

588 **Table 2**. Statistical indices for accessing the quantitative performance of non-rectangular
589 hyperbola (NRH), rectangular hyperbola (RH) and exponential (EXP) models describing the
590 irradiance response of photosynthesis when dark respiration (R_d) was estimated by the models
591 in ten tropical tree species in the non-flooding period (NFP) and flooding period (FP).

Species	**Non-rectangular hyperbola**						**Rectangular hyperbola**						**Exponential**					
	Non-flooding (*NFP*)			Flooding (*FP*)			Non-flooding (*NFP*)			Flooding (*FP*)			Non-flooding (*NFP*)			Flooding (*FP*)		
	r^2	*Aud(%)*	*RMSE*	r^2	*Aud(%)*	*RMSE*	r^2	*Aud(%)*	*RMSE*	r^2	*Aud(%)*	*RMSE*	r^2	*Aud(%)*	*RMSE*	r^2	*Aud(%)*	*RMSE*
N. amazonum	0.9903	27.8	0.496	0.994	22.9	0.450	0.999		0.166	0.999		0.175	0.997	12.8	0.343	0.997		0.313
M.angustifolium	0.9900	20.4	0.456	0.992	14.9	0.354	1.000	4.7	0.096	0.998	6.3	0.168	0.993	11.4	0.368	0.996	5.9	0.246
A. discolor	0.9990	31.3	0.595	0.990	20.9	0.482	0.999		0.153	0.999		0.114	0.993	20.9	0.487	0.998	15.5	0.396
								3.9			4.9							
B. lactescens	0.9975	28.3	0.605	0.984	21.6	0.440	0.994		0.300	0.998		0.130	0.977	24.4	0.578	0.988	16.5	0.392
								9.7			4.4							
S. reticulata	0.9997	33.7	0.623	0.996	17.8	0.661	0.999	15.4	0.284	1.000	5.5	0.184	0.999	5.0	0.246	0.999	4.5	0.270
G. sprucea na	0.9995	19.3	0.402	0.994	16.1	0.353	0.999		0.203	0.998		0.188	0.999		0.248	0.998		0.220
								6.4			6.2			8.8			6.9	
P. excelsa	0.9902	19.4	0.377	0.995	12.0	0.268	1.000		0.075	0.999		0.249	0.999	10.7	0.280	0.998		0.164
								3.4			9.9						3.3	
C. concolor	0.9966	26.9	0.541	0.975	17.8	0.211	0.999		0.249	0.999		0.051	0.999		0.244	0.984	12.0	0.177
								8.3			4.2			8.4				
V. guianensis	0.9887	17.1	0.523	0.972	16.1	0.128	0.999		0.133	0.989	10.2	0.081	0.999	10.3	0.456	0.983		0.099
								4.4									8.1	
V. japurensis	0.9881	31.4	0.587	0.971	16.7	0.150	0.996		0.257	0.999		0.032	0.984	24.7	0.545	0.987		0.100
								7.8			5.3						9.5	
Average	**0.990**	**25.6**	**0.520**	**0.986**	**17.7**	**0.350**	**0.998**	**6.9**	**0.192**	**0.998**	**6.2**	**0.136**	**0.993**	**13.8**	**0.379**	**0.992**	**9.2**	**0.238**

592 r^2 = coefficient of determination; *Aud*(%) = the average of unsigned deviation; *RMSE* = the
593 root mean square of error (*RMSE*).
594

Table 3. Measured and estimated photosynthesis maxima (P_{nmax}) from three models when dark respiration (R_d) was estimated by the models in ten tropical tree species in two flooding periods.

	Measured		**Non-rectangular hyperbola**				**Rectangular hyperbola**				**Exponential**		
	Non-flooding	Flooding	Non-flooding		Flooding		Non-flooding		Flooding		Non-flooding		Floodin
	Mean (min-max)	Mean (min-max)	%	r^2	%	r^2	%	r^2	%	r^2	%	r^2	%
num	**15.1** (11.6-19.3)	**14.2** (11.7-17.1)	38.5	0.888	36.1	0.766	16.4	0.995	16.2	0.998	-2.0	0.996	-1.9
ifolium	**11.9** (9.3-15.6)	**10.4** (7.5-13.0)	33.7	0.987	29.7	0.508	11.9	0.997	12.2	0.996	-3.5	0.998	-2.3
r	**14.4** (10.1-18.2)	**11.6** (6.5-16.9)	70.9	0.473	62.4	0.671	25.8	0.778	22.4	0.940	1.5	0.920	-0.1
ens	**10.4** (7.2-13.4)	**9.2** (5.9-10.9)	80.5	0.414	55.1	0.641	11.0	0.971	14.2	0.967	-3.2	0.995	-2.0
ata	**27.3** (24.8-30.1)	**26.6** (21.3-32.4)	43.3	0.754	49.5	0.525	31.1	0.877	36.9	0.945	3.1	0.974	5.2
ana	**14.4** (12.0-16.5)	**12.0** (10.5-15.3)	34.4	0.982	31.0	0.978	17.1	0.975	15.3	0.997	-1.5	0.993	-1.6
	11.1 (9.6-14.3)	**9.6** (7.1-12.9)	37.5	0.889	24.6	0.952	14.0	0.985	13.3	0.992	-2.4	0.994	-2.0
or	**22.8** (17.2-27.7)	**3.0** (0.1-9.3)	45.4	0.779	29.5	0.949	27.4	0.898	7.6	0.998	1.9	0.970	-6.8
nsis	**11.6** (7.7-16.1)	**1.5** (0.8-2.5)	43.2	0.671	20.7	0.818	16.3	0.861	10.0	0.972	-0.5	0.860	-2.7
nsis	**11.1** (7.8-13.1)	**2.1** (0.0-4.9)	59.0	0.639	7.3	0.988	16.6	0.876	5.2	0.998	-1.4	0.907	-4.9
s	**15.0 (7.2-30.1)**	**10.0 (0.0-32.4)**	**48.3**	**0.861**	**41.0**	**0.958**	**20.8**	**0.980**	**20.9**	**0.986**	**-0.2**	**0.992**	**-0.1**

Mean (min-max) of ten repetitions for each species in the non-flooding and flooding periods. The percentages (%) represent changes (positive or negative relative to measured values) that occurred in P_{nmax} estimated by the NRH, RH and EXP models. r^2 = coefficient of determination

Table 4. Measured and estimated dark respiration (R_d) by three models in ten tropical tree species in two flooding periods.

	Measured		**Non-rectangular hyperbola**				**Rectangular hyperbola**				**Exponential**		
	Non-flooding	Flooding	Non-flooding		Flooding		Non-flooding		Flooding		Non-flooding		Floodin
	Mean (min-max)	Mean (min-max)	%	r^2	%	r^2	%	r^2	%	r^2	%	r^2	%
num	**1.44** (0.77-2.51)	**1.37** (0.95-2.79)	-62.6	0.916	-60.5	0.955	16.2	0.890	18.4	0.893	-27.3	0.852	-23.8
ifolium	**0.61** (0.43-0.88)	**0.80** (0.43-1.04)	-128.9	0.412	-85.2	0.829	26.1	0.882	25.7	0.780	-56.1	0.240	-26.3
r	**1.73** (0.86-2.27)	**1.84** (1.19-2.69)	-60.2	0.891	-50.2	0.878	-9.0	0.680	-6.1	0.815	-37.9	0.777	-32.8
ens	**0.74** (0.45-1.17)	**0.83** (0.54-1.17)	-150.3	0.328	-104.7	0.655	-36.5	0.339	-20.5	0.509	-122.3	0.219	-74.8
ata	**1.63** (0.79-2.18)	**2.04** (1.32-2.67)	-67.4	0.903	-48.5	0.823	16.9	0.904	12.6	0.540	-21.6	0.880	-13.8
ana	**1.00** (0.59-1.45)	**0.78** (0.61-1.06)	-75.2	0.869	-86.5	0.761	29.1	0.969	32.4	0.833	-26.3	0.939	-22.4
	0.56 (0.30-1.03)	**0.72** (0.47-1.43)	-130.3	0.759	-67.6	0.252	20.4	0.810	42.8	0.714	-64.7	0.731	-9.0
or	**1.50** (0.99-2.49)	**0.97** (0.40-1.69)	-68.6	0.612	-38.4	0.682	15.7	0.601	1.7	0.921	-26.3	0.561	-13.8
nsis	**1.08** (0.77-1.48)	**0.88** (0.45-1.20)	-77.1	0.488	-25.0	0.963	10.0	0.664	5.5	0.907	-39.1	0.518	-2.6
nsis	**1.21** (0.70-2.04)	**0.68** (0.40-1.00)	-92.1	0.802	-45.8	0.637	-26.7	0.706	3.4	0.963	-71.6	0.730	-8.7
s	**1.15 (0.30-2.51)**	**1.09 (0.40-2.79)**	**-81.7**	**0.770**	**-58.3**	**0.692**	**5.8**	**0.749**	**9.9**	**0.839**	**-43.1**	**0.707**	**-23.0**

Mean (min-max) of ten repetitions for each species in the non-flooding and flooding periods. The percentages (%) represent changes (positive or negative relative to measured values) that occurred in R_d estimated by the NRH, RH and EXP models. r^2 = coefficient of determination.

Table 5. Measured values (including points of Kok-effect region) and estimated apparent quantum yield (α) by initial slope excluding points of Kok-effect region, and by the RH and EXP models when dark respiration (R_d) was estimated by the models in ten tropical tree species in two flooding periods.

	Measured		**Estimated excluding kok effect**				**Rectangular hyperbola**				**Exponential**		
	Non-flooding	Flooding	Non-flooding		Flooding		Non-flooding		Flooding		Non-flooding		Floodin
	Mean (min-max)	Mean (min-max)	%	r^2	%	r^2	%	r^2	%	r^2	%	r^2	%
num	**0.054** (0.047-0.061)	**0.052** (0.047-0.054)	-6.0	0.952	-6.0	0.916	53.8	0.209	57.8	0.166	2.8	0.247	5.9
folium	**0.048** (0.043-0.053)	**0.046** (0.038-0.053)	-6.5	0.918	-8.3	0.988	61.9	0.009	79.5	0.670	6.4	0.001	19.7
r	**0.047** (0.036-0.055)	**0.041** (0.030-0.052)	-9.6	0.952	-12.0	0.930	31.6	0.885	37.0	0.773	-9.5	0.862	-9.5
ens	**0.043** (0.033-0.054)	**0.036** (0.027-0.045)	-9.4	0.974	-12.3	0.926	24.6	0.034	36.2	0.818	-24.7	0.178	-13.8
ata	**0.058** (0.053-0.068)	**0.052** (0.045-0.059)	-7.0	0.626	-3.9	0.948	35.8	0.638	30.4	0.509	2.7	0.451	1.4
ana	**0.049** (0.043-0.067)	**0.044** (0.038-0.048)	-5.3	0.982	-6.7	0.884	56.5	0.946	65.1	0.580	6.0	0.952	12.9
	0.041 (0.034-0.052)	**0.041** (0.026-0.057)	-7.5	0.989	-4.6	0.975	54.4	0.832	79.4	0.808	1.2	0.786	20.6
or	**0.056** (0.047-0.066)	**0.020** (0.007-0.041)	-6.6	0.457	-15.6	0.993	38.2	0.317	117.5	0.774	0.4	0.304	38.7
nsis	**0.049** (0.038-0.057)	**0.017** (0.012-0.021)	-7.4	0.902	-13.9	0.781	56.5	0.637	184.2	0.013	2.9	0.509	73.5
nsis	**0.041** (0.033-0.049)	**0.018** (0.005-0.034)	-12.2	0.882	-22.6	0.994	21.7	0.665	147.5	0.753	-15.2	0.567	51.2
s	**0.049 (0.033-0.068)**	**0.037 (0.005-0.059)**	**-7.6**	**0.923**	**-8.9**	**0.986**	**43.8**	**0.572**	**70.0**	**0.607**	**-1.2**	**0.647**	**13.8**

Mean (min-max) of ten repetitions for each species in the non-flooding and flooding periods. The percentages (%) represent changes (positive or negative relative to measured values) that occurred in R_d estimated by the NRH, RH and EXP models. r^2 = coefficient of determination.

Table 6. Statistical indices for accessing the quantitative performance of non-rectangular hyperbola (NRH), rectangular hyperbola (RH) and exponential (EXP) models describing the irradiance response of photosynthesis, when measured dark respiration (R_d) was added in the models, in ten tropical species in non flooding (NFP) and flooding period (FP).

Species	**Non-rectangular hyperbola**						**Rectangular hyperbola**						**Exponential**					
	Non-flooding (*NFP*)			Flooding (*FP*)			Non-flooding (*NFP*)			Flooding (*FP*)			Non-flooding (*NFP*)			Flooding (*FP*)		
	Aud (%)	*RMSE*	r^2	*Aud (%)*	*RMSE*	r^2	*Aud (%)*	*RMSE*	r^2	*Aud (%)*	*RMSE*	r^2	*Aud (%)*	*RMSE*	r^2	*Aud (%)*	*RMSE*	*RMSE*
N. amazonum	0.987	40.8	0.705	0.988	35.6	0.641	0.999	12.3	0.189	0.999	12.1	0.202	0.996	15.2	0.387	0.996	12.2	0.344
M.angustifolium	0.981	15.0	0.622	0.984	15.9	0.510	0.999	3.6	0.114	0.998	5.8	0.186	0.992	6.2	0.397	0.996	4.6	0.260
A. discolor	0.977	55.6	0.878	0.976	40.7	0.740	0.999	10.6	0.176	0.999	8.0	0.136	0.989	35.6	0.621	0.988	25.7	0.520
B. lactescens	0.954	23.8	0.824	0.967	27.3	0.641	0.993	5.2	0.315	0.998	5.0	0.149	0.968	15.9	0.681	0.982	17.3	0.475
S. reticulata	0.993	52.5	0.924	0.993	27.2	0.908	0.999	4.3	0.310	1.000	6.9	0.223	0.999	21.0	0.310	0.999	7.4	0.309
G. sprucea na	0.990	19.9	0.586	0.988	16.5	0.515	0.998	9.0	0.232	0.998	6.4	0.206	0.998	5.8	0.277	0.997	5.3	0.244
P. excelsa	0.984	15.9	0.545	0.990	13.9	0.377	1.000	2.7	0.087	0.995	9.8	0.267	0.994	7.2	0.320	0.998	2.4	0.166
C. concolor	0.992	41.1	0.837	0.952	34.9	0.293	0.999	3.8	0.264	0.999	4.0	0.051	0.999	17.7	0.331	0.980	14.7	0.188
V. guianensis	0.976	21.7	0.697	0.959	27.2	0.155	0.999	4.6	0.137	0.988	10.3	0.082	0.988	9.9	0.491	0.983	7.7	0.099
V. japurensis	0.962	46.9	0.830	0.944	36.6	0.208	0.996	11.0	0.281	0.999	5.4	0.033	0.976	31.1	0.663	0.986	11.0	0.103
Average	**0.979**	**33.3**	**0.745**	**0.974**	**27.6**	**0.499**	**0.998**	**6.7**	**0.210**	**0.997**	**7.4**	**0.153**	**0.990**	**16.5**	**0.448**	**0.991**	**10.8**	**0.271**

r^2 = coefficient of determination; *Aud*(%) = the average of unsigned deviation; *RMSE* = the root mean square of error.

Table 7. Estimated photosynthesis maxima (P_{nmax}) from three models when measured dark respiration (R_d) was added to the models in ten tropical tree species in two flooding periods.

Species	Non-rectangular hyperbola				Rectangular hyperbola				Exponential			
	Non-flooding		Flooding		Non-flooding		Flooding		Non-flooding		Flooding	
	%	r^2	%	r^2	%	r^2	%	r^2	%	r^2	%	r^2
N. amazonum	22.0	0.962	20.4	0.930	17.2	0.994	17.0	0.998	-2.8	0.993	-2.6	0.983
M.angustifolium	17.0	0.993	13.4	0.869	12.4	0.997	12.5	0.993	-4.2	0.997	-3.1	0.984
A. discolor	42.5	0.622	32.2	0.912	23.1	0.886	21.3	0.951	-1.1	0.960	-2.5	0.985
B. lactescens	26.9	0.915	26.5	0.816	9.1	0.951	12.5	0.983	-7.6	0.954	-5.3	0.990
S. reticulata	32.1	0.805	37.5	0.711	32.3	0.833	38.0	0.968	2.5	0.957	4.5	0.992
G. spruceana	21.1	0.989	17.9	0.992	18.2	0.973	16.3	0.996	-1.9	0.991	-2.2	0.997
P. excelsa	19.7	0.964	12.8	0.967	14.4	0.984	14.3	0.990	-3.3	0.991	-2.2	0.988
C. concolor	32.2	0.814	33.2	0.977	28.3	0.902	7.6	0.997	1.2	0.968	-7.7	0.997
V. guianensis	20.9	0.824	7.4	0.842	16.5	0.852	10.3	0.970	-1.7	0.849	-3.0	0.977
V. japurensis	32.1	0.416	27.8	0.935	12.9	0.967	5.3	0.998	-6.0	0.990	-5.2	0.999
All species	**27.7**	**0.945**	**34.3**	**0.972**	**20.8**	**0.985**	**21.2**	**0.986**	**-1.6**	**0.993**	**-1.1**	**0.997**

* See Mean (min-max) of measured P_{nmax} in **Table 3**

** The percentages (%) represent changes (positive or negative relative to measured values) that occurred in P_{nmax} estimated by the NRH, RH and EXP models. r^2 = coefficient of determination.

Table 8. Estimated apparent quantum yield (α) from the RH and EXP models when measured dark respiration (R_d) was added to the models, in ten tropical tree species in two flooding periods.

Species	Rectangular hyperbola				Exponential			
	Non-flooding		Flooding		Non-flooding		Flooding	
	%	r^2	%	r^2	%	r^2	%	r^2
N. amazonum	45.6	0.314	47.9	0.256	11.8	0.380	13.8	0.273
M.angustifolium	53.8	0.042	67.1	0.630	16.9	0.055	26.0	0.678
A. discolor	33.5	0.884	42.3	0.706	2.8	0.892	9.4	0.741
B. lactescens	39.7	0.415	45.9	0.793	4.4	0.389	9.6	0.771
S. reticulata	30.7	0.881	25.4	0.696	7.0	0.834	4.6	0.706
G. spruceana	45.5	0.940	53.2	0.591	12.5	0.940	17.4	0.666
P. excelsa	48.4	0.917	61.8	0.903	13.0	0.927	23.6	0.913
C. concolor	33.1	0.578	114.7	0.820	6.3	0.633	53.0	0.907
V. guianensis	52.4	0.848	169.1	0.003	15.8	0.859	77.2	0.109
V. japurensis	37.0	0.828	142.6	0.874	2.3	0.744	59.1	0.928
All species	**41.7**	**0.696**	**64.7**	**0.653**	**9.4**	**0.773**	**23.6**	**0.808**

* See Mean (min-max) of measured α in **Table 5**

** The percentages (%) represent changes (positive or negative relative to measured values) that occurred in P_{nmax} estimated by the RH and EXP models. r^2 = coefficient of determination.

Table 9. Estimated convexity term (θ) by non-rectangular hyperbola when dark respiration (R_d) was estimated by the models, in ten tropical tree species in two flooding periods.

Species	Measured		Non-rectangular hyperbola			
	Non-flooding	Flooding	Non-flooding		Flooding	
	Mean (min-max)	Mean (min-max)	%	r^2	%	r^2
N. amazonum	**0.862** (0.824-0.909)	**0.869** (0.815-0.897)	5.4	0.783	5.1	0.903
M.angustifolium	**0.867** (0.827-0.906)	**0.890** (0.719-0.948)	5.9	0.973	5.2	0.960
A. discolor	**0.813** (0.713-0.922)	**0.816** (0.652-0.897)	7.1	0.947	9.2	0.302
B. lactescens	**0.761** (0.610-0.903)	**0.792** (0.578-0.893)	15.3	0.717	12.1	0.515
S. reticulata	**0.865** (0.839-0.883)	**0.860** (0.799-0.901)	3.2	0.720	3.1	0.994
G. spruceana	**0.872** (0.856-0.887)	**0.881** (0.864-0.918)	4.5	0.660	4.6	0.820
P. excelsa	**0.857** (0.831-0.888)	**0.904** (0.860-0.992)	6.2	0.897	4.1	0.971
C. concolor	**0.858** (0.822-0.889)	**0.908** (0.776-0.999)	3.9	0.679	1.5	0.611
V. guianensis	**0.858** (0.769-0.954)	**0.950** (0.811-0.994)	6.9	0.894	2.9	0.917
V. japurensis	**0.767** (0.610-0.852)	**0.966** (0.906-0.990)	13.5	0.864	3.3	0.105
All species	**0.838 (0.610-0.954)**	**0.884 (0.578-0.999)**	**7.0**	**0.7334**	**4.5**	**0.724**

Mean (min-max) of ten repetitions for each species in non-flooding and flooding periods. The percentages (%) represent changes (positive or negative relative to measured values) that occurred in θ estimated by the NRH model when R_d, was added to the model. r^2 = coefficient of determination

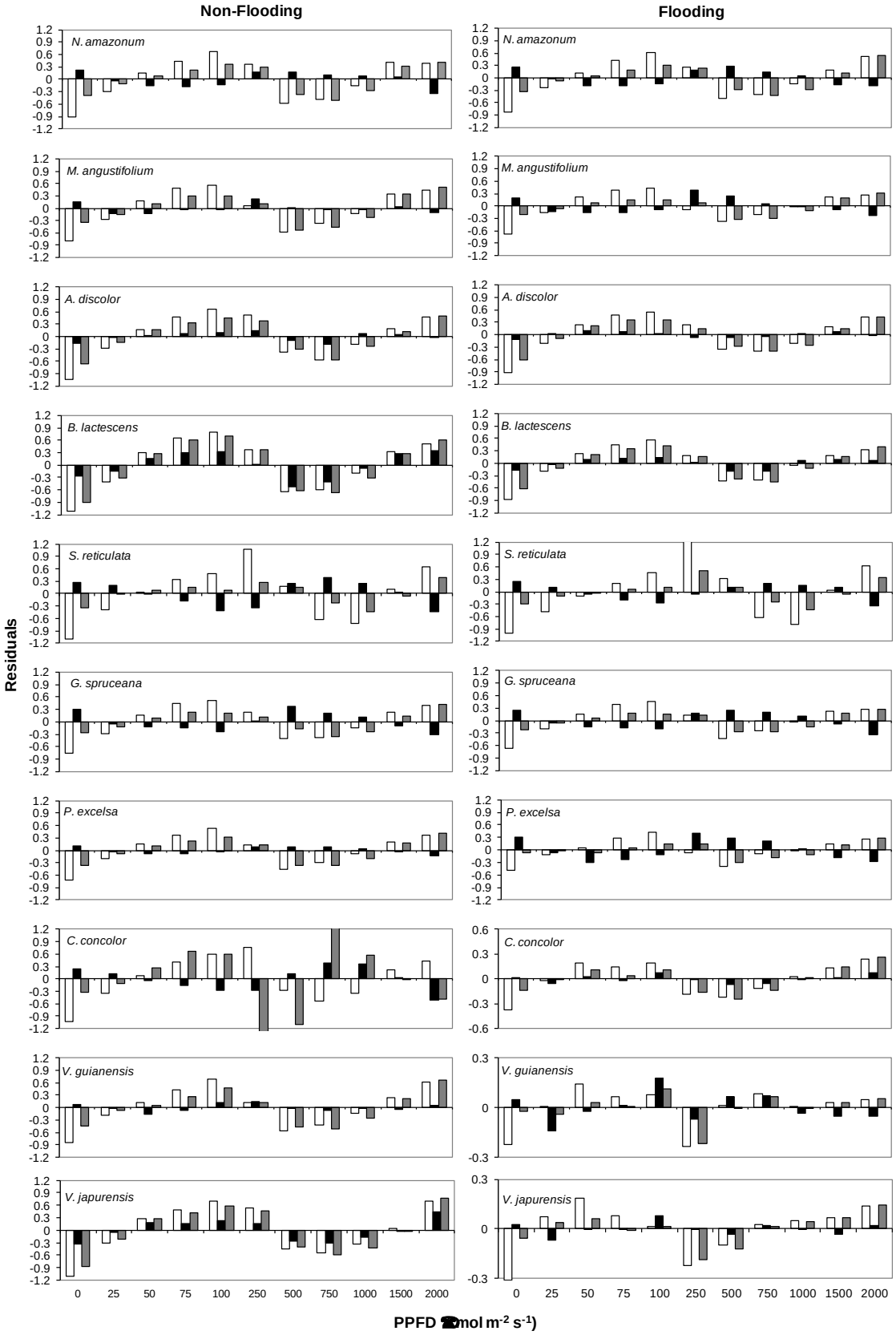
Non-Flooding
Flooding
N. amazonum
M. angustifolium
A. discolor
B. lactescens
S. reticulata
G. spruceana
P. excelsa
C. concolor
V. guianensis
V. japurensis
Residuals
PPFD (μmol m-2 s-1)
0 25 50 75 100 250 500 750 1000 1500 2000

Figure 1

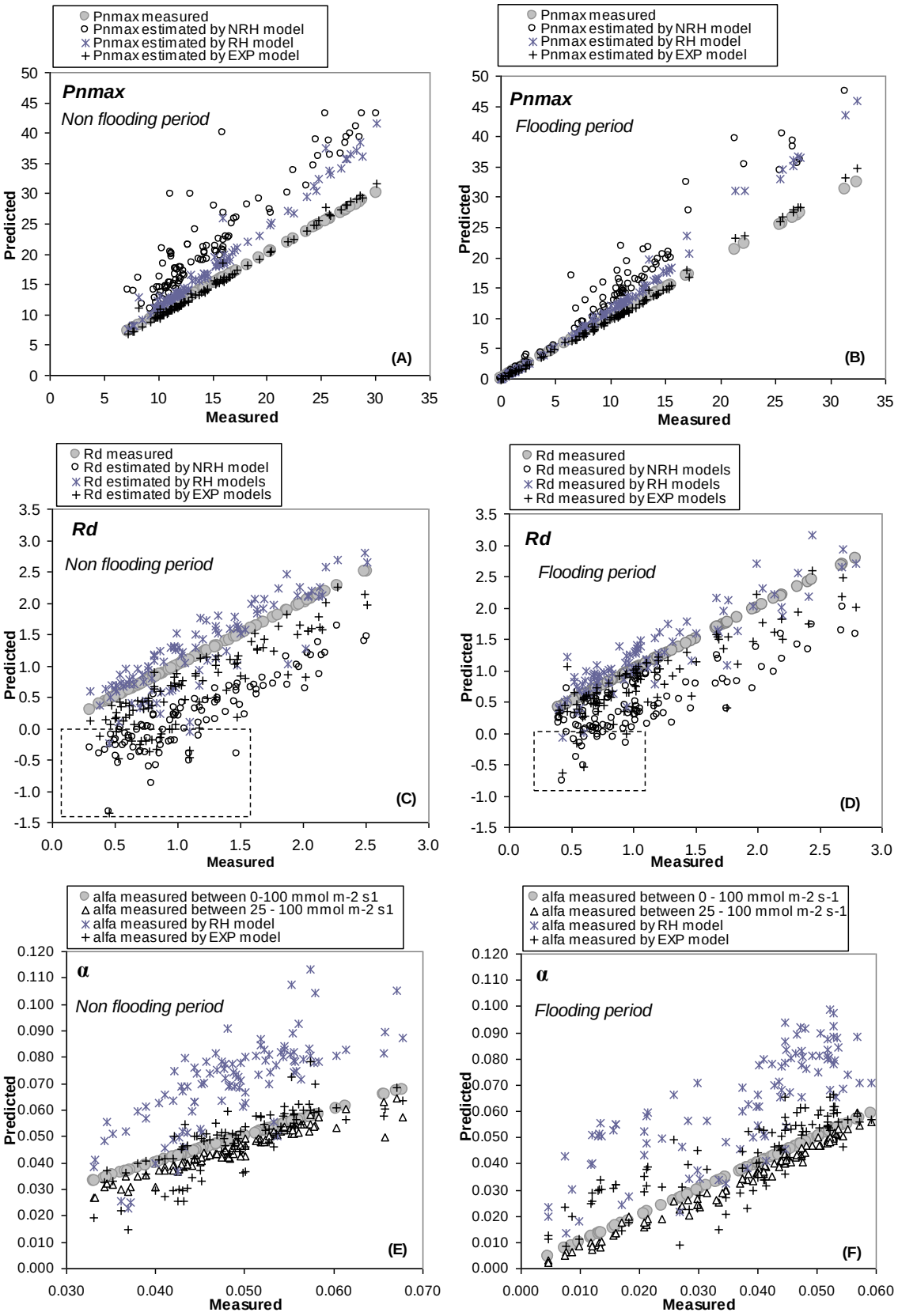
Pnmax measured
Pnmax estimated by NRH model
Pnmax estimated by RH model
Pnmax estimated by EXP model
Pnmax
Non flooding period
Predicted
Measured
(A)
Pnmax measured
Pnmax estimated by NRH model
Pnmax estimated by RH model
Pnmax estimated by EXP model
Pnmax
Flooding period
Predicted
Measured
(B)
Rd measured
Rd estimated by NRH model
Rd estimated by RH models
Rd estimated by EXP models
Rd
Non flooding period
Predicted
Measured
(C)
Rd measured
Rd measured by NRH models
Rd measured by RH models
Rd measured by EXP models
Rd
Flooding period
Predicted
Measured
(D)
alfa measured between 0-100 mmol m-2 s1
alfa measured between 25 - 100 mmol m-2 s1
alfa measured by RH model
alfa measured by EXP model
α
Non flooding period
Predicted
Measured
(E)
alfa measured between 0 - 100 mmol m-2 s-1
alfa measured between 25 - 100 mmol m-2 s-1
alfa measured by RH model
alfa measured by EXP model
α
Flooding period
Predicted
Measured
(F)

Figure 2

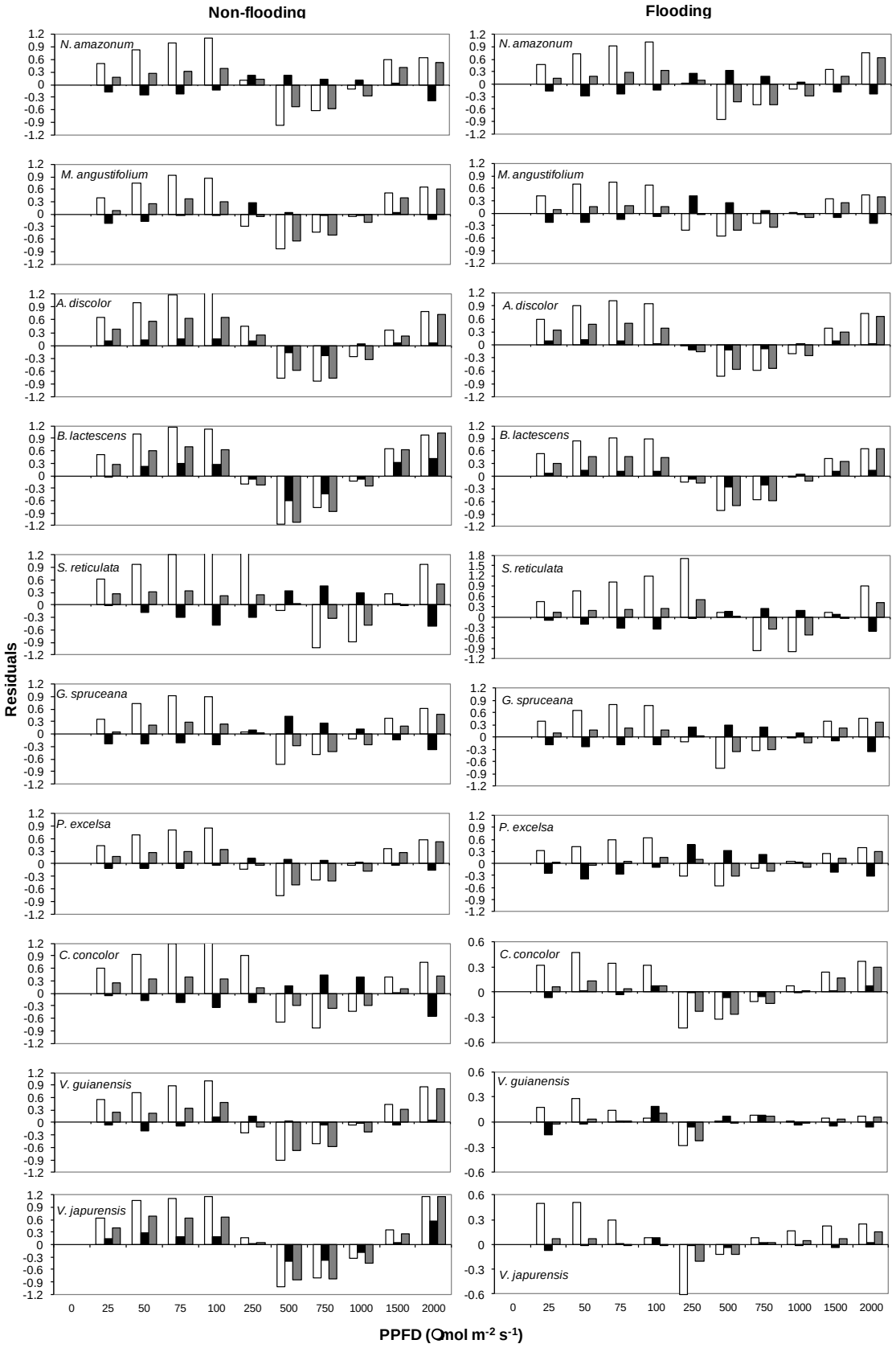
Non-flooding
Flooding
N. amazonum
M. angustifolium
A. discolor
B. lactescens
S. reticulata
G. spruceana
P. excelsa
C. concolor
V. guianensis
V. japurensis
Residuals
PPFD (Qmol m-2 s-1)
0 25 50 75 100 250 500 750 1000 1500 2000

Figure 3

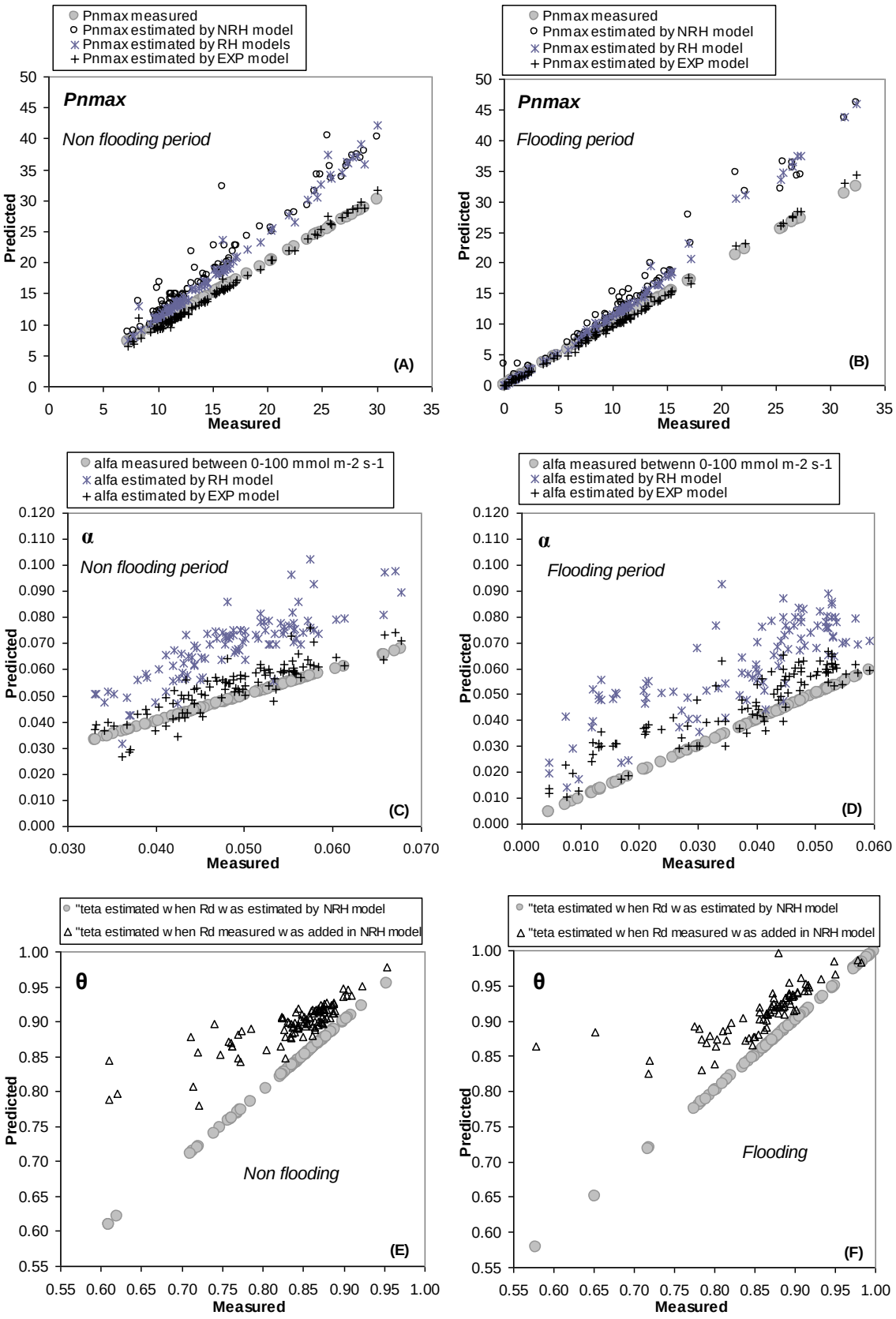
Pnmax measured
Pnmax estimated by NRH model
Pnmax estimated by RH models
Pnmax estimated by EXP model
Pnmax
Non flooding period
(A)
Predicted
Measured
Pnmax measured
Pnmax estimated by NRH model
Pnmax estimated by RH model
Pnmax estimated by EXP model
Pnmax
Flooding period
(B)
Predicted
Measured
alfa measured between 0-100 mmol m-2 s-1
alfa estimated by RH model
alfa estimated by EXP model
α
Non flooding period
(C)
Predicted
Measured
alfa measured betwenn 0-100 mmol m-2 s-1
alfa estimated by RH model
alfa estimated by EXP model
α
Flooding period
(D)
Predicted
Measured
"teta estimated when Rd was estimated by NRH model
"teta estimated when Rd measured was added in NRH model
θ
Non flooding
(E)
Predicted
Measured
"teta estimated when Rd was estimated by NRH model
"teta estimated when Rd measured was added in NRH model
θ
Flooding
(F)
Predicted
Measured

Figura 4